

# Optical Kerr Effect Spectroscopy Using Time-Delayed Pairs of Pump Pulses with Orthogonal Polarizations<sup>†</sup>

Xiang Zhu, Richard A. Farrer, and John T. Fourkas\*

Eugene F. Merkert Chemistry Center, Boston College, Chestnut Hill, Massachusetts 02467

Received: July 21, 2004; In Final Form: September 2, 2004

We characterize in detail a recently introduced technique in which perpendicularly polarized pulses with controllable intensities and timing are used for the excitation step in optical Kerr effect spectroscopy. We examine the ratio of pump pulse intensities required to cancel the contribution of reorientational diffusion or of a Raman-active intramolecular vibration to the signal as a function of the delay time between excitation pulses. These results indicate that the signal can be described well as arising from the sum of independent third-order responses initiated by each pump pulse. This conclusion is further supported by using data obtained with a single pump pulse to model decays obtained with two pump pulses.

## I. Introduction

Optical Kerr effect (OKE) spectroscopy has found broad use in monitoring ultrafast dynamics in transparent media.<sup>1–4</sup> In recent years, this technique has been applied to the study of simple,<sup>5–11</sup> supercooled,<sup>12–15</sup> ionic,<sup>16–18</sup> and confined<sup>19–22</sup> liquids, liquid mixtures,<sup>23–28</sup> polymers,<sup>22,29</sup> biomolecules,<sup>30–32</sup> and complex fluids.<sup>33–37</sup> Interest is also developing in using OKE spectroscopy as a means of achieving contrast in nonlinear microscopy.<sup>38</sup> Such contrast could in principle be based on any of the contributions to the OKE signal, which include electronic hyperpolarizability, impulsively excited intermolecular modes, impulsively excited, Raman-active intramolecular vibrations, and molecular reorientation. In practice, however, separating these different contributions from one another is often difficult due to a considerable degree of overlap in the time scales of the processes that are involved.

We have recently introduced a technique that allows for the selective enhancement or suppression of specific contributions to the OKE signal.<sup>39</sup> Our method draws its inspiration from the work of Weiner, Nelson, and co-workers,<sup>40–42</sup> who demonstrated that by employing trains of pulses with a spacing equal to the period of a specific Raman-active vibration for excitation the contribution of that mode to the OKE signal was strongly enhanced. While in that work all of the excitation pulses were of the same polarization, Wefers, Kawashima, and Nelson more recently demonstrated that with two perpendicularly polarized excitation pulses control could be exerted over the Raman-active lattice vibrations in crystalline quartz.<sup>43</sup> Gershgoren et al. have also demonstrated a related technique with electronically resonant, parallel-polarized pump pulses on  $\text{I}_3^-$  in solution.<sup>44</sup> We previously reported the application of a similar technique to liquids<sup>39</sup> and demonstrated that with two pump pulses with independently controllable timing, intensity, and polarization it is possible to suppress or enhance the contribution of a specific intramolecular vibrational mode or of reorientation to the OKE signal.

While it is possible to exert a considerable amount of control over the contributions to the OKE signal with just two pump

pulses, for microscopy and other applications ultimately it will be desirable to employ trains of pulses with arbitrary time delays, intensities, and polarizations to isolate the contributions of individual modes. To be able to design appropriate excitation pulse sequences, it is first necessary to develop a detailed understanding of the dual-pulse-excitation scheme. With that goal in mind, here we present a detailed study of the OKE spectroscopy of liquids using two perpendicularly polarized excitation pulses, and we demonstrate that the signal can be modeled well by the sum of two independent third-order responses.

## II. Theory

We begin by considering a conventional OKE experiment performed in an isotropic medium using a polarization-spectroscopy configuration, the interactions of which are shown schematically as a ladder diagram in Figure 1a. Excitation is accomplished with a single linearly polarized pump pulse, the polarization of which we will call  $x$ . The probe pulse, which arrives at some time  $\tau$  later, is polarized at  $45^\circ$  to the pump ( $(x + y)/\sqrt{2}$ ) and the signal at  $-45^\circ$  to the pump ( $(x - y)/\sqrt{2}$ ). The only nonzero tensor elements of the third-order response function in an isotropic medium are those in which each spatial index appears an even number of times. The response function measured in the polarization-spectroscopy geometry is therefore

$$R_{\text{PS}}^{(3)}(\tau) = \frac{1}{2}R_{\text{xxxx}}^{(3)}(\tau) - \frac{1}{2}R_{\text{yyxx}}^{(3)}(\tau) \quad (1)$$

where the subscript indices refer to the polarizations of the interactions in reverse temporal order. Furthermore, in an isotropic medium the relationships among the different tensor elements of the third-order response are such that<sup>45,46</sup>

$$\frac{1}{2}R_{\text{xxxx}}^{(3)}(\tau) - \frac{1}{2}R_{\text{yyxx}}^{(3)}(\tau) = R_{\text{xyxy}}^{(3)}(\tau) \quad (2)$$

This latter quantity is known as the depolarized response, and it arises solely from modes that affect the polarizability of the liquid anisotropically.

\* Author to whom correspondence should be addressed. E-mail: fourkas@bc.edu.

<sup>†</sup> Part of the special issue "George W. Flynn Festschrift".

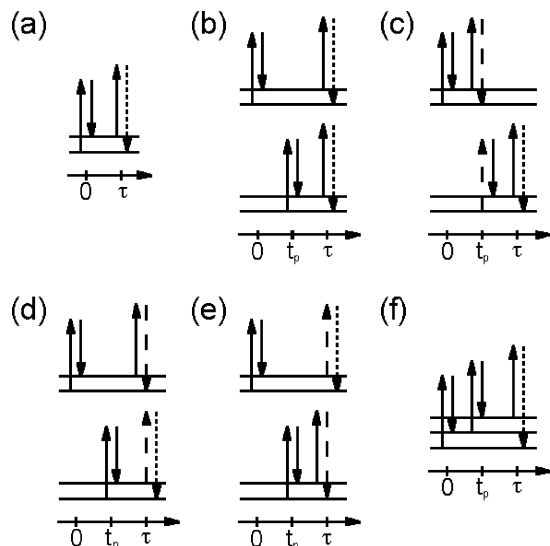


**Figure 1.** Ladder diagram representations of processes that contribute to the OKE decay with (a) one and (b–f) two pump pulses. Horizontal lines denote energy levels of Raman-active intermolecular and intramolecular modes of the liquid. In parts b–e, the pair of horizontal lines is involved in an independent third-order response. Solid vertical arrows indicate laser interactions, dotted arrows indicate signal fields, and dashed arrows indicate intermediate fields arising from a third-order response that act as one of the source fields for another third-order response. The diagram in part b illustrates the case of two independent third-order responses, part c shows a serial cascade, parts d and e are parallel cascades, and part f is a representative pathway in the fifth-order nonresonant response.

Now consider the use of two orthogonally polarized pump pulses that are not time coincident (Figure 1b). We will assume that the first pulse is *x*-polarized and arrives at time zero and that the second pulse is *y*-polarized and arrives at time  $t_p$ . The intensity of the second pump pulse is  $a$  times that of the first. The probe pulse is again polarized at  $45^\circ$  and arrives at time  $\tau$ , and detection is performed at  $-45^\circ$ . We will constrain ourselves to the case in which none of the pulses overlap in time and  $\tau > t_p$ . Under these circumstances, there are three possible contributions to the signal, all of which are phase-matched. The first type of contribution is the sum of the independent third-order responses from each of the pump beams with the probe beam. The response function in the case of independent responses is given by

$$R_{-ddy\bar{x}}^{(3+3)}(t_p, \tau) = R_{xyxy}^{(3)}(\tau) - aR_{xyxy}^{(3)}(\tau - t_p) \quad (3)$$

where we have taken advantage of the fact that  $R_{xyxy}^{(3)} = R_{yyxx}^{(3)}$  in an isotropic medium. Here the superscript of the response denotes that it is the sum of two third-order responses, and the subscript gives the polarizations of the pump beams, the probe beam, and the signal beam in reverse temporal order;  $d$  denotes a polarization of  $45^\circ$ , and  $-d$  denotes a polarization of  $-45^\circ$ .

From eq 3, it is straightforward to see how mode selectivity might be achieved. We consider in particular two contributions to the depolarized response, that from orientational diffusion and that from coherently excited intramolecular vibrations. For symmetric top molecules,<sup>47</sup> the former contribution is given by

$$R_{xyxy, \text{reor}}^{(3)}(\tau) \propto \exp(-\tau/\tau_r) \quad (4)$$

where  $\tau_r$  is the collective orientational correlation time. Inspection of eqs 3 and 4 shows that if  $a$  is chosen to be  $\exp(-t_p/\tau_r)$ , then

$$R_{-ddy\bar{x}, \text{reor}}^{(3+3)}(t_p, \tau) \propto \exp(-\tau/\tau_r) - \exp(-t_p/\tau_r) \exp(-(\tau - t_p)/\tau_r) = 0 \quad (5)$$

and so the reorientational contribution to the signal can be canceled. In a similar vein, the contribution to the depolarized response from a coherently excited intramolecular vibration, in the limit of exponential damping, is given by

$$R_{xyxy, \text{vib}}^{(3)}(\tau) \propto \exp(-\tau/\tau_v) \sin(\omega\tau) \quad (6)$$

where  $\omega$  is the frequency of the vibration and  $\tau_v$  is its damping time. Combining eqs 3 and 6 and choosing  $a$  to be equal to  $\exp(-t_p/\tau_v)$ , we find that

$$R_{-ddy\bar{x}, \text{vib}}^{(3+3)}(t_p, \tau) \propto \exp(-\tau/\tau_v) \sin(\omega\tau) - \exp(-t_p/\tau_v) \exp(-(\tau - t_p)/\tau_v) \sin(\omega(\tau - t_p)) \\ = \exp(-\tau/\tau_v) [\sin(\omega\tau) - \sin(\omega\tau - \varphi)] \quad (7)$$

where  $\varphi = \omega t_p$ . If the phase is chosen to be  $2n\pi$ , where  $n$  is an integer, then the contribution from an intramolecular vibration can be canceled completely, and so long as  $\tau_r$  is not equal to  $\tau_v$ , there will still be a reorientational signal. Conversely, if the phase is chosen to be  $(2n + 1)\pi$ , then the vibrational signal will instead be enhanced, regardless of the choice of  $a$ .

The second potential contribution to the signal arises from cascaded third-order processes,<sup>48,49</sup> of which there are two possible cases, serial and parallel. In the former case (Figure 1c), the second pump pulse acts as a probe pulse for the coherence created by the first pump pulse. The resultant third-order signal field then acts as one pump field for an ensuing third-order process. Within the polarization scheme used here, the response arising from the serial cascade follows

$$R_{-ddy\bar{x}}^{(3,3,s)}(t_p, \tau) \propto \frac{a}{2} R_{yyxx}^{(3)}(t_p) (R_{xyxy}^{(3)}(\tau - t_p) - R_{yyxy}^{(3)}(\tau - t_p)) = \\ aR_{yyxx}^{(3)}(t_p) R_{xyxy}^{(3)}(\tau - t_p) \quad (8)$$

where the superscript on the response function denotes that it arises from a serial cascade of two third-order responses. In the latter case, the signal electric field generated from one pump pulse and the probe pulse acts as a pump field for the coherence generated by the other pump pulse. There are two ways in which such a parallel cascaded signal can be generated (Figure 1, parts d and e), and here both pathways yield an identical response. The total response from the parallel cascade is given by

$$R_{-ddy\bar{x}}^{(3,3,p)}(t_p, \tau) \propto 2a(R_{xxxx}^{(3)}(\tau) R_{xyxy}^{(3)}(\tau - t_p) - R_{yyxx}^{(3)}(\tau) R_{yyxy}^{(3)}(\tau - t_p)) \\ = 2a(R_{xxxx}^{(3)}(\tau) R_{xyxy}^{(3)}(\tau - t_p) - R_{xyxy}^{(3)}(\tau) R_{xxxx}^{(3)}(\tau - t_p)) \quad (9)$$

where the superscript on the response function denotes that it arises from a parallel cascade of two third-order responses.

The final potential contribution to the signal arises from a direct fifth-order response.<sup>50</sup> A number of different pathways contribute to this response, and one representative such pathway is shown in Figure 1f. The relevant fifth-order response in this case is given by

$$R_{-ddy\bar{x}}^{(5)}(t_p, \tau) = R_{xyxyxx}^{(5)}(t_p, \tau - t_p) - R_{yyxyxx}^{(5)}(t_p, \tau - t_p) \quad (10)$$

The total response function, which is measured directly when optical heterodyne detection is employed, is given by the sum

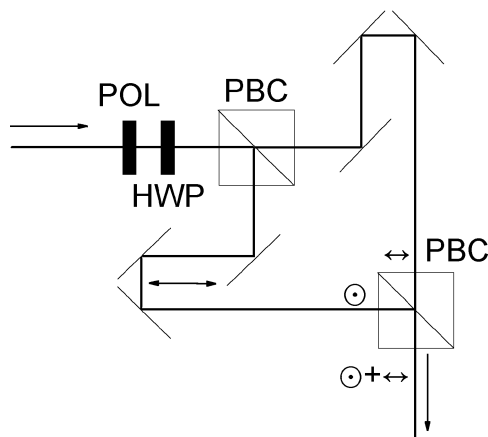


**Figure 2.** Experimental setup for creating perpendicularly polarized pump pulses with independently adjustable intensities and timing. POL = polarizer, HWP = half-wave plate, and PBC = polarizing beam cube. The symbols near the second PBC denote the polarizations in each leg and at the output of the interferometer.

of the individual contributions

$$R_{-ddy}^{(\text{total})}(t_p, \tau) = R_{-ddy}^{(3+3)}(t_p, \tau) + R_{-ddy}^{(3,3,s)}(t_p, \tau) + R_{-ddy}^{(3,3,p)}(t_p, \tau) + R_{-ddy}^{(5)}(t_p, \tau) \quad (11)$$

Thus, in general the total response could be quite complex. However, the fifth-order response is known to be many orders of magnitude smaller than the cascaded third-order responses<sup>49</sup> and so can safely be ignored. It is further expected that the cascaded third-order responses should be significantly weaker than the sum of individual third-order responses, since the electric field from any individual third-order response would normally be much weaker than the electric field of any of the laser pulses. It is still possible that the cascaded response could be appreciable, however. To distinguish the sum of individual third-order responses from that of cascaded third-order responses, we note that in the former case the temporal behavior of the signal depends explicitly on the relative intensities of the pump pulses, whereas in the latter case it does not. Furthermore, in the case of serial cascades the response function is the product of two third-order response functions, so it is not possible to cancel vibrational or reorientational contributions to this response by adjusting the delay and amplitudes of the pump pulses. The response from parallel cascades is necessarily zero when  $\tau = 2t_p$ , but it is otherwise not generally possible to cancel the vibrational or reorientational contributions to this response by adjusting the delay and amplitudes of the pump pulses.

### III. Experimental Section

Our experimental setup is similar to the one used in our previous work on OKE spectroscopy with multiple pump pulses<sup>39</sup> but differs in some details. A commercial Ti:sapphire laser (KMLabs TS) pumped by a frequency-doubled, diode-pumped solid-state laser (Coherent Verdi 5) produces 50 fs pulses with a center wavelength of 800 nm and a repetition rate of 90 MHz. The output of the laser is sent through a prism dispersion compensator and a spatial filter, after which it is split into a pump beam and a weaker probe beam. The two pump pulses are then created by the optical setup shown in Figure 2. A half-wave plate is used to rotate the polarization of the beam, after which it is split into beams of orthogonal polarization by a polarizing beam cube. The timing of one beam is adjusted

with an optical delay line, and the beams are recombined at a second polarizing beam cube and focused into the sample. The input wave plate can be used to adjust the relative intensities of the pump beams, and if beams of the same polarization are desired, then a half-wave plate and a polarizer can be placed between the second polarizing beam cube and the sample.

The probe beam traverses an optical delay line, after which it passes through a Glan-laser polarizer set to pass light polarized at 45° and then through a quarter-wave plate along the fast axis. The beam is then focused into the sample with the same lens that focuses the pump beam. After the sample, the probe beam is sent into a polarizer set to pass light polarized at -45°, following which it is spatially filtered and sent to a low-noise amplified photodiode. The first polarizer in the probe beam path is turned slightly (~1°) to create a local oscillator for optical heterodyne detection, and opposite angular displacements of the polarizer are used in consecutive scans. The difference between averaged data sets at opposite heterodyne angles yields the pure heterodyne signal.

The pump and probe beams are chopped by different rings of the same chopper wheel at frequencies that are in a 7:5 ratio. A portion of the probe beam is picked off after the chopper and sent to a reference photodiode that is identical to the one that detects the signal. The outputs of the two photodiodes are connected to the differential inputs of a low-noise preamplifier (SRS SR560). The two signals are balanced carefully with the pump beam blocked so that the preamplifier output is as close to zero as possible. The preamplifier output is then sent to a digital lock-in amplifier (SRS SR810) that is referenced to the sum of the chopping frequencies. The pump beam is picked off after the sample and frequency-doubled. The doubled light is detected by another photodiode and lock-in amplifier; this signal is used to normalize for any long-term intensity fluctuations of the laser.

All of the liquids were filtered before use and, if necessary, were distilled. Samples were placed in cuvettes with a 1 mm path length and mounted to a three-axis translation stage. The lab temperature was constant to within ±1 °F for all experiments, so no additional temperature control for the samples was deemed necessary.

### IV. Results

We begin by considering the suppression of the contribution of reorientational diffusion in the OKE decay of a simple liquid. Shown in Figure 3 (black line) is the OKE decay of benzene at room temperature after a single pump pulse. As can be seen in the semilogarithmic plot in the inset of this figure, the OKE decay features a long exponential tail. This tail, which has a time constant  $\tau_r$  of 3.03 ps,<sup>5</sup> arises from the diffusive decay of the orientational anisotropy created by the probe pulse.

The red line in Figure 3 shows a benzene OKE decay in which perpendicularly polarized pump pulses have been employed. For this particular set of data, the delay between the pump pulses was 133 fs. Note that the decay becomes negative in sign around the time of arrival of the second pump pulse and remains so for all subsequent delay times, as is predicted by eq 3 so long as the intensity of the second pump pulse is great enough relative to that of the first pump pulse. If desired, the sign of the decay can be flipped by using a negative value of  $t_p$ . For these data, the intensity ratio of the pump pulses was chosen to optimize the suppression of the contribution of reorientational diffusion. As can be seen in the inset of this figure, the diffusive contribution to the decay is smaller than the noise in the signal and so has been suppressed by more

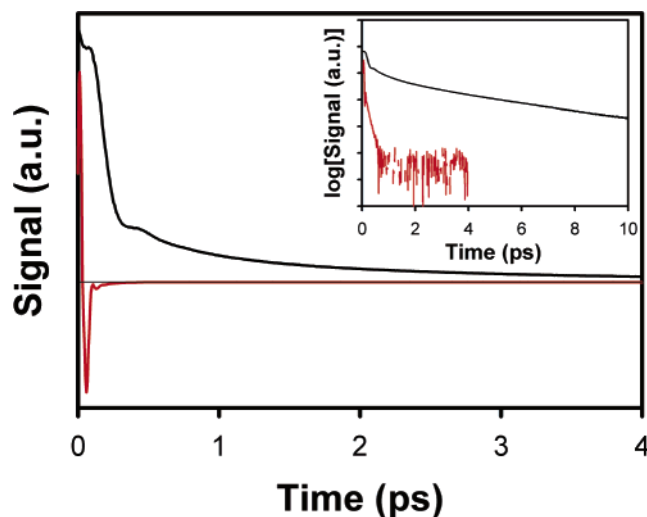


**Figure 3.** OKE decays for room-temperature benzene with one pump pulse (black line) and two perpendicularly polarized pump pulses separated by 133 fs (red line). The horizontal line demarcates the zero level of the signal. Shown in the inset is a semilogarithmic plot of the data with single-pulse excitation (black line) and the negative of the data two-pulse excitation (red line). The tick marks on the ordinate are factors of 10. The bottom of the inset is the approximate zero level of the spectra.

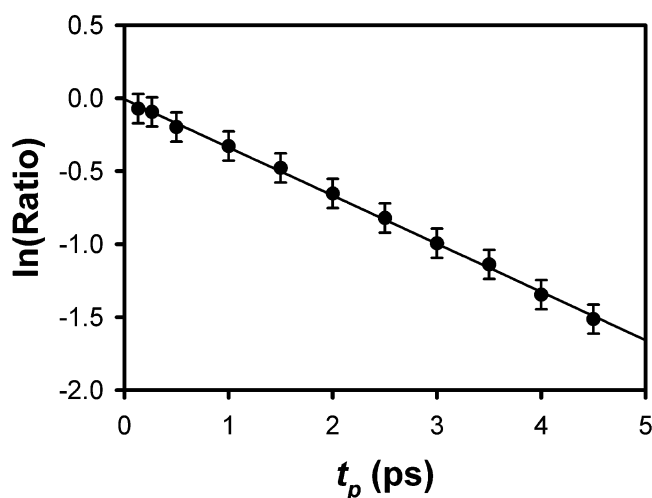


**Figure 4.** Ratio of pump beam intensities required to cancel the orientational diffusion component of the benzene OKE decay as a function of  $t_p$ . The solid line is a linear least-squares fit to the data.

than three and a half orders of magnitude. If the ratio of the intensities of the pump pulses is made either larger or smaller than the optimal value, then the diffusive decay becomes visible again. The greater the deviation of the ratio from the optimal value, the greater is the amplitude of diffusive decay.

According to eq 5, the ratio of pump pulse intensities needed to suppress the reorientational contribution to the data completely should scale as  $\exp(-t_p/\tau_r)$ . To test this prediction, we measured the ratio of intensities needed to suppress this contribution for values of  $t_p$  ranging from 133 fs to 4.5 ps. The results of these experiments are plotted in semilogarithmic form in Figure 4. The intensity ratio is clearly an exponential function of  $t_p$ . A linear least-squares fit of the data yields a slope of  $-0.33 \text{ ps}^{-1}$ , which is identical to the value of  $-1/\tau_r$ .

These results are consistent with the signal being dominated by the sum of two third-order responses. The shape of the decay changes with the ratio of pump pulse intensities, and the ratio of intensities required to suppress the orientational contribution to the signal follows the behavior predicted for the sum of

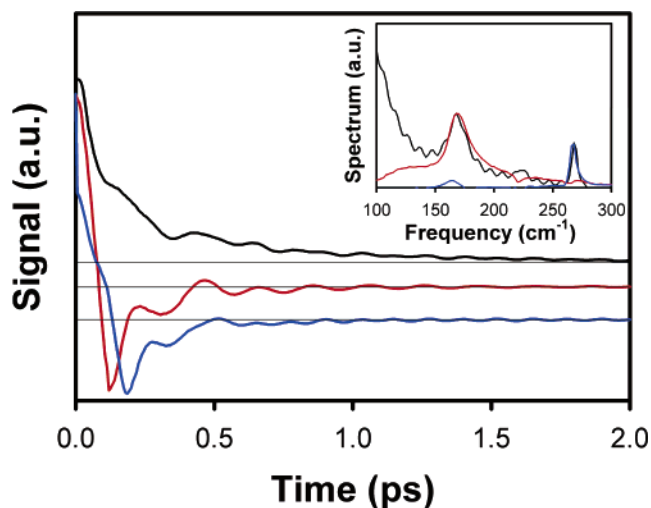


**Figure 5.** OKE decays for iodobenzene at room temperature. The black line is the data for a single pump pulse, the red line is the data for pump pulses separated by one period of the higher-frequency vibration (122 fs), and the blue line is the data for pump pulses separated by one period of the lower-frequency vibration (200 fs). The horizontal lines demarcate the zero level of the signal. The inset shows part of the imaginary portion of the Fourier transform of each decay, demonstrating the excellent mode suppression when dual pump pulses are employed.

responses. It is also worth note that the predicted behavior is followed even when the separation between the pump pulses is so short as to lie within the portion of the response that is dominated by intermolecular modes, as in Figure 3.

We now turn to the suppression of the contributions of specific intramolecular vibrational modes. Shown in Figure 5 is the OKE decay for iodobenzene at room temperature (black line). The inset shows the imaginary portion of the Fourier transform of these data from 100–300  $\text{cm}^{-1}$ . There are two depolarized, Raman-active intramolecular vibrations within the bandwidth of the laser, one at 167  $\text{cm}^{-1}$  and one at 273  $\text{cm}^{-1}$ .

Also shown in Figure 5 are OKE decays for iodobenzene that has been excited with perpendicularly polarized pump pulses. In the red decay, the delay between pump pulses was set to 122 fs, one period of the higher-frequency vibration. In the blue decay,  $t_p$  was set to 200 fs, one period of the lower-frequency mode. For each data set, the relative intensities of the pump pulses were adjusted to optimize the suppression of the mode of interest. It can be seen in the inset of Figure 5 that in both cases the contribution of the suppressed vibrations is greatly reduced.

To examine the intensity ratio of the pump pulses that is needed to suppress an intramolecular vibrational mode, we turn to the case of chloroform. Shown as a black line in Figure 6 is the OKE decay for chloroform at room temperature for a single pump pulse. As can be seen in the inset spectrum, two Raman-active intramolecular modes contribute to the decay, a strong one at 262  $\text{cm}^{-1}$  and a weaker one at 365  $\text{cm}^{-1}$ . The red line in Figure 6 is the OKE decay resulting from the use of two perpendicularly polarized pump pulses separated by one period of the 262  $\text{cm}^{-1}$  vibration (127 fs). As can be seen in the inset, under these conditions the contribution from this vibration is strongly suppressed.

According to eq 7, the intensity ratio needed to cancel the contribution of a vibration when  $t_p$  is an integral number of periods of the vibration should scale as  $\exp(-t_p/\tau_r)$ . To test this prediction, we first obtained an OKE decay in which the mode at 365  $\text{cm}^{-1}$  was suppressed. The portion of this decay after



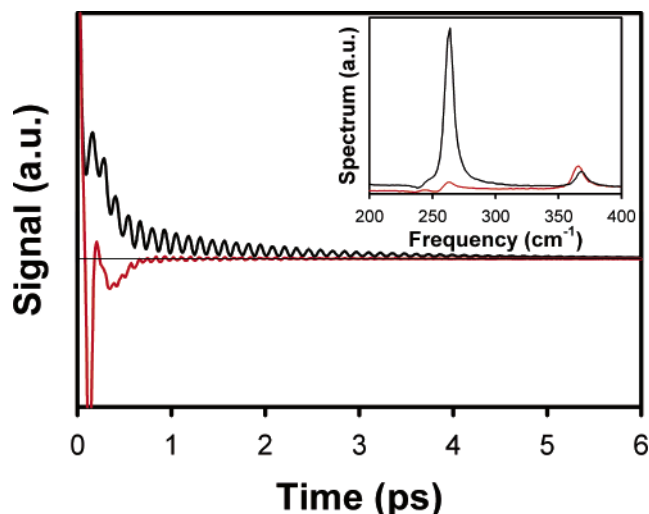


**Figure 6.** Room-temperature OKE decays for chloroform with a single pump pulse (black line) and with two perpendicularly polarized pump pulses separated by one period (127 fs) of the lower-frequency vibrational mode (red line). The horizontal line demarcates the zero level of the signal. Shown in the inset are part of the imaginary portions of the Fourier transforms of the two decays. The bottom of the inset is the approximate zero level of the spectra.

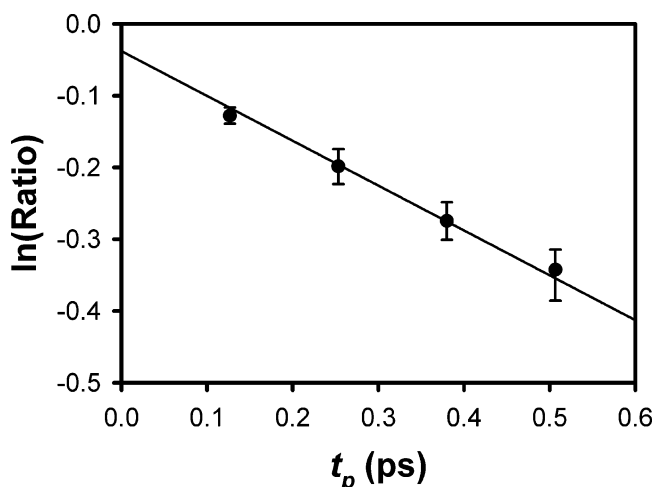


**Figure 7.** Ratio of pump beam intensities required to suppress the contribution of the 262 cm<sup>-1</sup> mode in the OKE decay of chloroform as a function of  $t_p$ . The line is a linear least-squares fit to the data in which the slope has been constrained to be the logarithm of the dephasing rate of the vibration.

the intermolecular modes had damped out was then fit to the equation

$$S(\tau) = A \exp(-\tau/\tau_r) + B \exp(-\tau/\tau_v) \sin(\omega_v \tau) \quad (12)$$

where  $A$  and  $B$  are amplitudes,  $\tau_r$  is the collective orientational correlation time (which we have previously measured<sup>5</sup> to be 3.28 ps at room temperature), and  $\omega_v$  and  $\tau_v$  are the angular frequency and dephasing time of the 262 cm<sup>-1</sup> vibration. On the basis of this fit, the vibrational dephasing time was determined to be 1.6 ps. We next measured the ratio of pump intensities required to suppress this mode for values of  $t_p$  that were integer multiples of the period of the vibration. These data are plotted in semilogarithmic form in Figure 7. The solid line is the result of a linear least-squares fit in which the slope has been constrained to be the negative inverse of  $\tau_v$ . The fit is in good agreement with the data, which further supports the sum of independent third-order responses model for the signal.

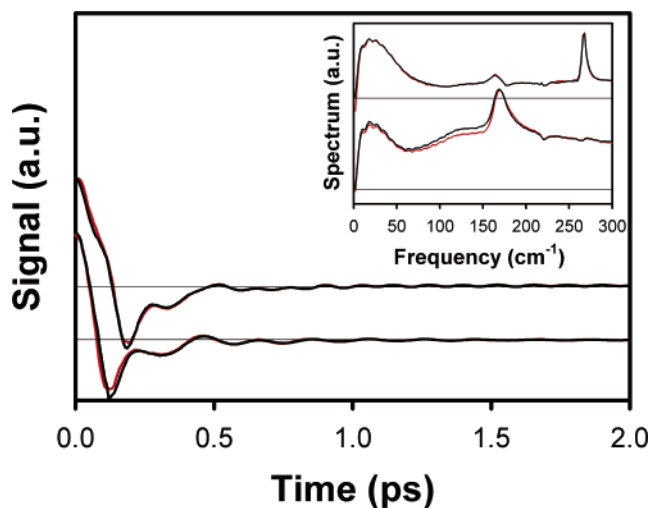


**Figure 8.** The black lines are OKE decays for room-temperature iodobenzene. In the upper data set, the lower-frequency vibration has been suppressed ( $t_p = 122$  fs), and in the lower data set, the higher-frequency vibration has been suppressed ( $t_p = 200$  fs). The red lines are simulations of the decays that are derived from the single-pulse excitation data. The horizontal lines demarcate the zero level of the signal and the approximate zero levels of the spectra. As can be seen from the decays and from the inset with the corresponding spectra, the agreement between the data and the simulation is excellent.

As an additional check of the sum of independent responses model, we can test eq 3 directly by using the OKE decay with a single pump pulse to model the decay from perpendicular pump pulses. The signal from a single pump pulse is time shifted by  $t_p$ , multiplied by the ratio of the intensity of the second pump pulse to the first, and then subtracted from the signal from a single pump pulse. Shown in Figure 8 is the result of this procedure for the perpendicularly polarized pump OKE decays for iodobenzene from Figure 5. As can be seen from the time-domain data and from the imaginary portion of their Fourier transforms in the inset, the model gives a good fit to the data. The fit is particularly good for the case in which the 167 cm<sup>-1</sup> mode is suppressed, but both data sets offer strong support for the signal arising predominantly from the sum of independent third-order responses. We have obtained equally good results in using eq 3 to simulate the perpendicularly polarized pump pulse OKE decays for all of the other liquids studied here.

A potentially important application of mode-selective OKE spectroscopy is the isolation of the signal of a single component in a mixture. With this thought in mind, we used perpendicularly polarized pump pulses to study the OKE response of a 1:1 (v/v) mixture of chloroform and chlorobenzene. As discussed above, chloroform has an intramolecular vibration at 262 cm<sup>-1</sup> that contributes strongly to its OKE signal. Chlorobenzene, however, has a strong depolarized Raman-active mode at 199 cm<sup>-1</sup>. As shown in the decays and the inset spectra in Figure 9, when the separation between the pump pulses is one period of the chloroform mode (128 fs), its contribution is strongly suppressed. The same is true for the chlorobenzene mode when the pump pulses are separated by 172 fs. Even when the liquids are in volume ratios as large as 20:1, we have found that it is possible to suppress the vibrational contribution of the major component so that it is significantly smaller than that of the minor component.

In the results presented up to now, we have suppressed the contributions of a vibrational mode by separating the two pump pulses by a single period of the vibration. However, if one wishes to suppress one mode while maximally enhancing

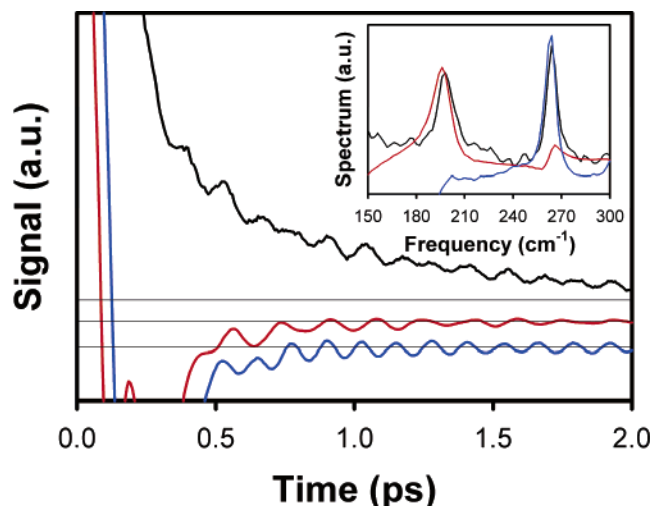


**Figure 9.** OKE decays for a 1:1 v/v mixture of chloroform and chlorobenzene. The black line is the decay for a single pump pulse. Two pump pulses have been used to suppress the chlorobenzene mode at 199  $\text{cm}^{-1}$  in the red decay ( $t_p = 128$  fs) and to suppress the chloroform mode at 262  $\text{cm}^{-1}$  in the blue decay ( $t_p = 172$  fs). The horizontal lines demarcate the zero level of the signal. The inset spectra demonstrate the quality of the mode suppression. The bottom of the inset is the approximate zero level of the spectra.

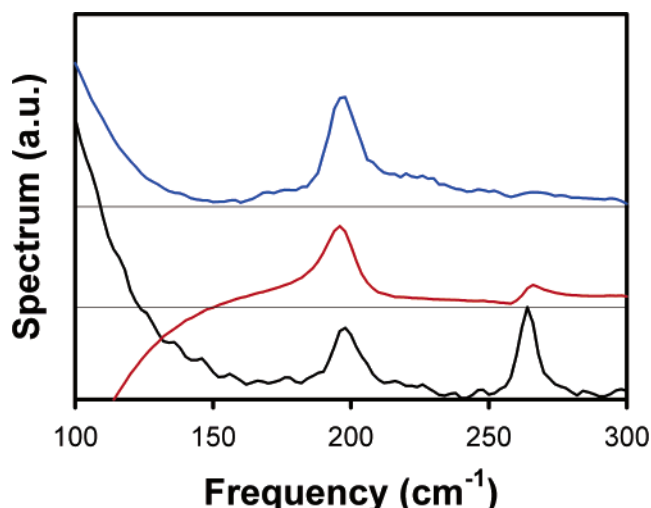


**Figure 10.** Imaginary portion of the Fourier transform of OKE decays in a 1:1 mixture of chloroform and chlorobenzene. The black spectrum is for a single pump pulse, the red spectrum is for pump pulses separated by 128 fs, and blue spectrum is for pump pulses separated by 256 fs. The spectra have been offset for clarity, and the horizontal lines denote the approximate zero levels.

another, then it may be desirable to separate the pump pulses by some other judiciously chosen integer multiple of the period. The mixture of chloroform and chlorobenzene is a case in point. Two periods of the 262  $\text{cm}^{-1}$  chloroform mode is 256 fs, whereas 1.5 periods of the chlorobenzene mode is 258 fs. Thus, separating the pump pulses by 256 fs not only serves to cancel the chloroform mode but is nearly optimal for enhancing the chlorobenzene mode as well. Shown in Figure 10 is a comparison of the imaginary portion of the Fourier transform of OKE data in a 1:1 mixture of chloroform and chlorobenzene with a single pump pulse, with two pump pulses separated by 128 fs and with two pump pulses separated by 256 fs. As expected, the spectral discrimination is strongest for the 256 fs separation between the pump pulses.

## V. Discussion

In symmetric top liquids, we have shown that it is possible to suppress the reorientational contribution to the signal completely by selecting appropriate intensities for the pump pulses at a given value of  $t_p$ . Since the use of perpendicularly polarized pump pulses will always tend to suppress the reorientational contribution to the signal, this latter contribution is also weakened considerably in all of the examples above in which we manipulate the strength of intramolecular vibrational contributions.

The complete suppression of reorientation becomes more difficult when molecules that are not symmetric tops are employed, however, since the reorientational decay is no longer described by a single exponential. However, the fact that the signal can be modeled to a high degree of accuracy by the sum of independent third-order responses from each pump pulse suggests that it will be straightforward to accomplish complete suppression of the reorientational contribution in more complex situations with the use of a larger number of pump pulses. Consider, for instance, a liquid composed of molecules with a polarizability tensor that has the same principal axes as its diffusion tensor but that has different diffusion constants about the principal axes of the latter tensor. In this case, the reorientational portion of the OKE decay is expected to be described by the sum of two exponentials<sup>47</sup> with amplitudes  $a_1$  and  $a_2$  and time constants  $\tau_{r1}$  and  $\tau_{r2}$ . We can use three pump pulses, with intensities  $A_1$ ,  $A_2$ , and  $A_3$ , to prepare this system. Pulse 1 is vertically polarized and arrives at time zero, pulse 2 is horizontally polarized and arrives at time  $t_{p1}$ , and pulse 3 is vertically polarized and arrives at time  $t_{p2}$ . Within the sum of independent responses model, the reorientational portion of the OKE response at probe delay  $\tau > t_{p2}$  is then given by

$$R_{xyxy, \text{reor}}^{(3)}(\tau) \propto A_1(a_1 e^{-\tau/\tau_{r1}} + a_2 e^{-\tau/\tau_{r2}}) - A_2(a_1 e^{-(\tau-t_{p1})/\tau_{r1}} + a_2 e^{-(\tau-t_{p2})/\tau_{r2}}) + A_3(a_1 e^{-(\tau-t_{p2})/\tau_{r1}} + a_2 e^{-(\tau-t_{p2})/\tau_{r2}}) \quad (13)$$

The only way for this response to be zero for all times  $\tau > t_{p2}$  is for the contribution from each reorientational component to be zero. Collecting the terms for each component, we find that

$$1 - B_2 e^{t_{p1}/\tau_{r1}} + B_3 e^{t_{p2}/\tau_{r1}} = 0 \quad (14)$$

and

$$1 - B_2 e^{t_{p1}/\tau_{r2}} + B_3 e^{t_{p2}/\tau_{r2}} = 0 \quad (15)$$

where  $B_n = A_n/A_1$ . These two equations are satisfied when

$$B_2 = \frac{e^{t_{p2}/\tau_{r1}} - e^{t_{p2}/\tau_{r2}}}{e^{t_{p2}/\tau_{r1}} e^{t_{p1}/\tau_{r2}} - e^{t_{p1}/\tau_{r1}} e^{t_{p2}/\tau_{r2}}} \quad (16)$$

and

$$B_3 = \frac{e^{t_{p1}/\tau_{r1}} - e^{t_{p1}/\tau_{r2}}}{e^{t_{p2}/\tau_{r1}} e^{t_{p1}/\tau_{r2}} - e^{t_{p1}/\tau_{r1}} e^{t_{p2}/\tau_{r2}}} \quad (17)$$

Note that these intensities are independent of the amplitudes of the two exponential decays,  $a_1$  and  $a_2$ . The generalization of this result is that an orientational decay composed of  $n$  exponentials can be canceled completely by  $n + 1$  pulses of appropriate intensities.

A parallel argument can be made for the suppression of vibrational modes, i.e., in general it should be possible to suppress the contributions of  $n$  vibrational modes completely

with a sequence of  $n + 1$  pulses. This strategy differs somewhat from that of Weiner, Nelson, and co-workers, who used trains of evenly spaced pulses of a single polarization to enhance a particular vibrational mode selectively, without the need to design the sequences to suppress other modes at the same time.<sup>40–42</sup> Given a tractable number of vibrational modes, employing a strategy that combines both enhancement and suppression would be desirable. However, when a large number of depolarized modes are present, focusing solely on enhancement of the mode of interest is the preferable approach. One key issue in this regard is that pulse trains that are significantly longer than the dephasing time of a vibration offer diminishing returns in enhancement. This situation can be improved upon by incorporating perpendicular polarizations into the excitation scheme. Rather than exciting with  $n$  pulses of the same polarization that are spaced by the period of the vibration,  $n/2$  pulses of one polarization could be alternated with  $n/2$  pulses of the orthogonal polarization. The pulses of each polarization would still be spaced by the vibrational period, but there would be a half-period offset between the two polarizations. In this manner, the total duration of the pulse sequence would be halved, which should lead to a significant improvement in excitation efficiency given the same integrated excitation intensity. Techniques for the simultaneous temporal and polarization shaping of ultrafast pulses should make such pulse sequences straightforward to implement.<sup>51</sup>

It is also worthwhile to compare our technique with other OKE techniques that take advantage of noncollinear pump beams with controllable polarizations to generate selective responses.<sup>52–54</sup> This other type of technique takes advantage of the symmetry properties of the third-order response tensor to suppress different contributions to the OKE signal. However, this type of technique relies on creating linear combinations of different tensor elements of the response at the same delay time. In contrast, our technique creates linear combinations of the same tensor element of the response at different delay times. Thus, while our technique can suppress the contribution of specific modes, the other type of technique necessarily suppresses every contribution that has the same tensor symmetry, e.g., all depolarized modes, all isotropic modes, or the electronic hyperpolarizability.

The technique that we have described here allows for the selective enhancement and suppression of particular contributions to the OKE signal. However, some of the remaining contributions to the signal, particularly those from intermolecular vibrational modes, may be distorted as compared to what is seen with a single pump pulse. As a result, using multiple pump pulses is not desirable in all circumstances. For instance, when two pump pulses are used, Fourier transform deconvolution<sup>55</sup> cannot be employed to derive the intermolecular spectrum.

One situation in which this new technique is useful is when oscillations from intramolecular vibrations overwhelm a reorientational decay. One application of particular interest to us is OKE microscopy. OKE spectroscopy shares many of the advantages of other nonlinear optical techniques that have been used for microscopy recently, including high spatial and temporal resolution and the ability to image in three dimensions. However, the potentially large number of contributions to the OKE signal can have a deleterious effect on contrast. By enhancement of the strength of a chosen contribution while others are suppressed, our technique may provide the means for increasing the contrast and the signal-to-noise ratio of OKE microscopy considerably, and this is an application that we will be pursuing soon.

## VI. Conclusions

In this paper, we have further explored a technique that we introduced recently in which a pair of perpendicularly polarized pump pulses is used in the excitation step of an OKE experiment in a polarization-spectroscopy geometry. We have shown that this scheme allows for the essentially complete suppression of the contribution of reorientational diffusion or of a selected vibrational mode to the OKE signal. Studies of the ratio of intensities of pump pulses required to cancel the contribution of reorientation or a specific vibration as a function of the delay time between the pump pulses are in good agreement with the signal arising from the sum of an independent third-order response originating with each pump pulse. Simulations of the signal from two pump pulses based on the signal with a single pump pulse further supports this picture. These experiments pave the way for using sequences of multiple pump pulses with controllable polarization, timing, and intensity to single out the contribution of a single mode of interest in a complex OKE decay. Such a technique would be of great interest for performing mode-selective OKE microscopy, among other applications.

**Acknowledgment.** This work was supported by the National Science Foundation, Grant CHE-0314020. J.T.F. is a Research Corporation Cottrell Scholar and a Camille Dreyfus Teacher–Scholar.

## References and Notes

- (1) Righini, R. *Science* **1993**, 262, 1386.
- (2) Kinoshita, S.; Kai, Y.; Ariyoshi, T.; Shimada, Y. *Int. J. Mod. Phys. B* **1996**, 10, 1229.
- (3) Fourkas, J. T. Nonresonant Intermolecular Spectroscopy of Liquids. In *Ultrafast Infrared and Raman Spectroscopy*; Fayer, M. D., Ed.; Marcel Dekker: New York, 2001; Vol. 26, p 473.
- (4) Smith, N. A.; Meech, S. R. *Int. Rev. Phys. Chem.* **2002**, 21, 75.
- (5) Loughnane, B. J.; Scodinu, A.; Farrer, R. A.; Fourkas, J. T.; Mohanty, U. *J. Chem. Phys.* **1999**, 111, 2686.
- (6) McMorow, D.; Lotshaw, W. T.; Kenney-Wallace, G. A. *IEEE J. Quantum Electron.* **1998**, 24, 443.
- (7) McMorow, D.; Thantu, N.; Kleiman, V.; Melinger, J. S.; Lotshaw, W. T. *J. Phys. Chem. A* **2001**, 105, 7960.
- (8) Castner Jr., E. W.; Maroncelli, M. *J. Mol. Liq.* **1998**, 77, 1.
- (9) Cong, P.; Deuel, H. P.; Simon, J. D. *Chem. Phys. Lett.* **1995**, 240, 72.
- (10) Neelakandan, M.; Pant, D.; Quitevis, E. L. *J. Phys. Chem. A* **1997**, 101, 2936.
- (11) Bartolini, P.; Ricci, M.; Torre, R.; Righini, R.; Santa, I. *J. Chem. Phys.* **1999**, 110, 8653.
- (12) Cang, H.; Novikov, V. N.; Fayer, M. D. *Phys. Rev. Lett.* **2003**, 90, 197401.
- (13) Cang, H.; Novikov, V. N.; Fayer, M. D. *J. Chem. Phys.* **2003**, 118, 2800.
- (14) Ricci, M.; Wiebel, S.; Bartolini, P.; Taschin, A.; Torre, R. *Philos. Mag. B* **2004**, 84, 1491.
- (15) Torre, R.; Bartolini, P.; Righini, R. *Nature* **2004**, 428, 296.
- (16) Cang, H.; Li, J.; Fayer, M. D. *J. Chem. Phys.* **2003**, 119, 13017.
- (17) Giraud, G.; Gordon, C. M.; Dunkin, I. R.; Wynne, K. *J. Chem. Phys.* **2003**, 119, 464.
- (18) Hyun, B. R.; Dzyuba, S. V.; Bartsch, R. A.; Quitevis, E. L. *J. Phys. Chem. A* **2002**, 106, 7579.
- (19) Loughnane, B. J.; Farrer, R. A.; Scodinu, A.; Reilly, T.; Fourkas, J. T. *J. Phys. Chem. B* **2000**, 104, 5421.
- (20) Farrer, R. A.; Fourkas, J. T. *Acc. Chem. Res.* **2003**, 36, 605.
- (21) Hunt, N. T.; Jaye, A. A.; Meech, S. R. *J. Phys. Chem. B* **2003**, 107, 3405.
- (22) Hunt, N. T.; Jaye, A. A.; Hellman, A.; Meech, S. R. *J. Phys. Chem. B* **2004**, 108, 100.
- (23) McMorow, D.; Thantu, N.; Melinger, J. S.; Kim, S. K.; Lotshaw, W. T. *J. Phys. Chem.* **1996**, 100, 10389.
- (24) Steffen, T.; Meinders, N. A. C. M.; Duppen, K. *J. Phys. Chem. A* **1998**, 102, 4213.
- (25) Idrissi, A.; Ricci, M.; Bartolini, P.; Righini, R. *J. Chem. Phys.* **2001**, 114, 6774.
- (26) Hunt, N. T.; Meech, S. R. *Chem. Phys. Lett.* **2003**, 378, 195.

- (27) Scodinu, A.; Fourkas, J. T. *J. Phys. Chem. B* **2003**, *107*, 44.
- (28) Wiewior, P. P.; Shirota, H.; Castner, E. W. *J. Chem. Phys.* **2002**, *116*, 4643.
- (29) Shirota, H.; Castner, E. W. *J. Am. Chem. Soc.* **2001**, *123*, 12877.
- (30) Eaves, J. D.; Fecko, C. J.; Stevens, A. L.; Peng, P.; Tokmakoff, A. *Chem. Phys. Lett.* **2003**, *376*, 20.
- (31) Giraud, G.; Wynne, K. *J. Am. Chem. Soc.* **2002**, *124*, 12110.
- (32) Giraud, G.; Karolin, J.; Wynne, K. *Biophys. J.* **2003**, *85*, 1903.
- (33) Cang, H.; Li, H.; Fayer, M. D. *Chem. Phys. Lett.* **2002**, *366*, 82.
- (34) Gottke, S. D.; Cang, H.; Bagchi, B.; Fayer, M. D. *J. Chem. Phys.* **2002**, *116*, 6339.
- (35) Gottke, S. D.; Brace, D. D.; Cang, H.; Bagchi, B.; Fayer, M. D. *J. Chem. Phys.* **2002**, *116*, 360.
- (36) Hyun, B. R.; Quitevis, E. L. *Chem. Phys. Lett.* **2003**, *373*, 526.
- (37) Hunt, N. T.; Meech, S. R. *J. Chem. Phys.* **2004**, *120*, 10828.
- (38) Potma, E. O.; de Boeij, W. P.; Wiersma, D. A. *Biophys. J.* **2001**, *80*, 3019.
- (39) Zhu, X.; Farrer, R. A.; Gershgoren, E.; Kapteyn, H. C.; Fourkas, J. T. *J. Phys. Chem. B* **2004**, *108*, 3384.
- (40) Weiner, A. M.; Leaird, D. E.; Wiederrecht, G. P.; Nelson, K. A. *Science* **1990**, *247*, 1317.
- (41) Weiner, A. M.; Leaird, D. E.; Wiederrecht, G. P.; Nelson, K. A. *J. Opt. Soc. Am. B* **1991**, *8*, 1264.
- (42) Wiederrecht, G. P.; Dougherty, T. P.; Dhar, L.; Nelson, K. A.; Weiner, A. M.; Leaird, D. E. *Ferroelectrics* **1993**, *144*, 1.
- (43) Wefers, M. M.; Kawashima, H.; Nelson, K. A. *J. Chem. Phys.* **1998**, *108*, 10248.
- (44) Gershgoren, E.; Vala, J.; Kosloff, R.; Ruhman, S. *J. Phys. Chem. A* **2001**, *105*, 5081.
- (45) Hellwarth, R. W. *Prog. Quantum Electron.* **1977**, *5*, 1.
- (46) Murry, R. L.; Fourkas, J. T. *J. Chem. Phys.* **1997**, *107*, 9726.
- (47) Berne, B. J.; Pecora, R. *Dynamic Light Scattering*; Wiley: New York, 1976.
- (48) Ulness, D. J.; Kirkwood, J. C.; Albrecht, A. C. *J. Chem. Phys.* **1998**, *108*, 3897.
- (49) Blank, D. A.; Kaufman, L. J.; Fleming, G. R. *J. Chem. Phys.* **1999**, *111*, 3105.
- (50) Tanimura, Y.; Mukamel, S. *J. Chem. Phys.* **1993**, *99*, 9496.
- (51) Brixner, T.; Gerber, G. *Opt. Lett.* **2001**, *26*, 557.
- (52) Etchepare, J.; Kenney-Wallace, G. A.; Grillon, G.; Migus, A.; Chambaret, J. P. *IEEE J. Quantum Electron.* **1982**, *QE-18*, 1826.
- (53) Etchepare, J.; Grillon, G.; Chambaret, J. P.; Hamoniaux, G.; Orszag, A. *Opt. Commun.* **1987**, *63*, 329.
- (54) Deeg, F. W.; Fayer, M. D. *J. Chem. Phys.* **1989**, *91*, 2269.
- (55) McMorow, D.; Lotshaw, W. T. *J. Phys. Chem.* **1991**, *95*, 10395.